SLAC-PUB-15275
KIAS-PREPRINT-P12062

Resummation of relativistic corrections to exclusive productions of charmonia in e^+e^- collisions

Ying Fan,[1,*] Jungil Lee,[1,†] and Chaehyun Yu[2,3,‡]

[1] *Department of Physics, Korea University, Seoul 136-701, Korea*

[2] *School of Physics, KIAS, Seoul 130-722, Korea*

[3] *SLAC National Accelerator Laboratory, 2575 Sand Hill Rd, Menlo Park, CA 94025, USA*

Abstract

We investigate two exclusive processes, $e^+e^- \to \eta_c + \gamma$ and $e^+e^- \to J/\psi + J/\psi$, at the center-of-momentum energy $\sqrt{s} = 10.58$ GeV within the framework of the nonrelativistic QCD factorization approach. A class of relativistic corrections is resummed to all orders in the heavy-quark velocity v and the corrections are large negative. We further improve the prediction by including available QCD next-to-leading-order corrections and the interference between the QCD and relativistic corrections. The prediction for $\sigma[e^+e^- \to \eta_c + \gamma]$ is about 50 fb. In the case of $e^+e^- \to J/\psi + J/\psi$ the standard nonrelativistic QCD prediction for the cross section is negative. As an alternative, the vector-meson-dominance approach is employed to compute the photon-fragmentation contribution of the process, which gives the cross section ~ 1 fb. This is an indication that the uncalculated QCD higher-order corrections may be significant. Our results can be tested against the forthcoming data from Belle II and super B factories.

PACS numbers: 12.38.Bx,12.38.Cy,12.39.St,14.40.Pq

* ying.physics.fan@gmail.com
† jungil@korea.ac.kr
‡ chyu@kias.re.kr

Published in arXiv:1211.4111

Work supported by US Department of Energy contract DE-AC02-76SF00515 and KIAS.

I. INTRODUCTION

The nonrelativistic QCD (NRQCD) factorization approach [1] is a systematic theoretical tool to study the production and decay of heavy quarkonia. In this approach, the production rate for a heavy quarkonium in a high-energy process is expressed as a linear combination of NRQCD long-distance matrix elements (LDMEs) for a heavy-quark-antiquark ($Q\bar{Q}_n$) pair into the physical quarkonium H. The velocity-scaling rules of NRQCD classify the numerical importance of each LDME relative to the color-singlet one in powers of v, the velocity of the quark and antiquark in the $Q\bar{Q}_n$ rest frame. The corresponding short-distance factors are calculable perturbatively. While the production of a quarkonium in hadron colliders involves various channels with the $Q\bar{Q}_n$ pair whose quantum number n differs from that of H, an exclusive quarkonium production process in e^+e^- annihilation such as $e^+e^- \to J/\psi + \eta_c$ or $e^+e^- \to J/\psi + J/\psi$ is dominated by the color-singlet process in which a produced $Q\bar{Q}$ pair has the same quantum number as that of a final-state quarkonium. This greatly reduces theoretical uncertainties. The factorization theorem for some exclusive quarkonium production processes in e^+e^- annihilation is available [2], although that for the inclusive quarkonium production is still a conjecture.

The only exclusive quarkonium production process that has been observed at B factories is $e^+e^- \to J/\psi + \eta_c$ [3]. Right after the first observation, it was revealed that the measured production rate [3] is greater than the leading-order (LO) NRQCD results [4, 5] by an order of magnitude. Although the subsequent measured values have decreased [6, 7] in comparison with the first measurement, the discrepancy still remained. Through extensive theoretical studies on the corrections at the next-to-leading order (NLO) in the strong coupling α_s [8] and the resummed relativistic corrections [9, 10], it was found that the interplay of the large QCD and relativistic corrections fill the gap between the theory and data [11–13] within uncertainties. A recent result for the order-$\alpha_s v^2$ corrections also supports this conclusion [14]. However, some subtle issues that should be clarified still exist: The current experimental data for $e^+e^- \to J/\psi + \eta_c$ contain the events with a $\mu^+\mu^-$ pair plus at least two charged tracks as the decay product of the η_c. If we take into account the η_c decay modes without charged tracks, then the actual cross section can be larger than the current data. While the size of the relativistic corrections has been estimated rather precisely with the aid of the resummation technique, the QCD corrections were computed only at order

α_s. The amount of higher-order (HO) QCD corrections are not estimated yet.

Another interesting issue is regarding the color-singlet LDMEs. The color-singlet LDMEs are usually determined by comparing experimental data with theoretical predictions for the electromagnetic decays of the S-wave charmonia, $J/\psi \to l^+l^-$ and $\eta_c \to \gamma\gamma$. It is known that the relativistic corrections to the charmonium decay rates are significant. In order to determine the color-singlet LDMEs including the relativistic corrections to these electromagnetic decays, we need at least two constraints for each decay rate. One is the experimental decay rate. As for the other constraint, one may choose the generalized Gremm-Kapustin relation [10] that relates the LDMEs of LO and HO [15–18]. As an alternative, one can use the measured rate $\Gamma[J/\psi \to \mathrm{LH}]$ for the J/ψ decay into light hadrons (LH) [13]. However, the numerical values for the LDMEs have a strong dependence on the choice: The LO LDME for J/ψ at $m_c = 1.4\,\mathrm{GeV}$ is $0.440\,\mathrm{GeV}^3$ [15] and $0.573\,\mathrm{GeV}^3$ [13]. The corresponding values for v^2 are 0.225 [15] and 0.089 [13]. Therefore, the phenomenological study on the exclusive quarkonium production rate in e^+e^- annihilation may provide us with a good chance of improving the accuracies in the determination of the color-singlet LDMEs. An accurate determination of the color-singlet LDMEs may lead to improving the determinations of various color-octet LDMEs that are involved in the inclusive productions of J/ψ [19].

One may also consider exclusive S-wave quarkonium processes in e^+e^- annihilation other than the observed one $e^+e^- \to J/\psi+\eta_c$. In Refs. [20, 21], the process $e^+e^- \to J/\psi+J/\psi$ was first introduced as a possible source of contaminating the data samples for $e^+e^- \to J/\psi+\eta_c$. The angular-distribution analysis of the $e^+e^- \to J/\psi + \eta_c$ events at Belle showed that there were no such contaminations. In addition, the Belle Collaboration has not observed the signals for $e^+e^- \to J/\psi + J/\psi$ yet and only an upper bound of the cross section has been reported: $\sigma[e^+e^- \to J/\psi + J/\psi] \times \mathcal{B}_{>2}[J/\psi] < 9.1$ fb [6]. According to the QCD NLO correction in Ref. [22], the NLO corrected cross section is significantly smaller than the LO prediction. As is stated in Refs. [20, 21], the process is dominated by the photon fragmentation. The relativistic and QCD corrections to this contribution can be summed effectively by making use of the vector-meson-dominance (VMD) approach [23]. The cross section within the VMD approach is $\sigma[e^+e^- \to J/\psi + J/\psi] = 1.69 \pm 0.35\,\mathrm{fb}$ at the center-of-momentum (CM) energy $\sqrt{s} = 10.58\,\mathrm{GeV}$ [23], which is significantly smaller than the LO prediction and is consistent with the nonobservation of the process at Belle. The production of a charge-conjugation parity $+1$ quarkonium associated with a photon, $e^+e^- \to H+\gamma$, was first suggested in Ref. [24] as a nice probe to the color-singlet mechanism of NRQCD and the convergence of relativistic corrections, especially for $\eta_c(2S)$. Later, both the QCD NLO and relativistic corrections to this process were calculated and found to be considerable [25, 26].

In this work, we investigate the resummed relativistic correction and its interplay with the QCD NLO correction to the exclusive processes $e^+e^- \to \eta_c + \gamma$ and $e^+e^- \to J/\psi + J/\psi$ at $\sqrt{s} = 10.58\,\mathrm{GeV}$. Because the QCD NLO and relativistic corrections to $e^+e^- \to J/\psi + \eta_c$ are large, one may guess that the two processes listed above may also acquire significant corrections relative to the LO contribution. Our calculation reveals that the corrections are indeed large negative. The resummation of relativistic corrections enhances the cross section for $e^+e^- \to \eta_c + \gamma$ in comparison with the order-v^2 relativistic correction. In the case of $e^+e^- \to J/\psi + J/\psi$, the QCD NLO and relativistic corrections resummed to all orders in v make the cross section negative within the standard NRQCD factorization approach. By employing the VMD approach to compute the photon-fragmentation contribution, we cure the problem. The result shows that the QCD HO corrections may have significant contributions to $e^+e^- \to J/\psi + J/\psi$. Therefore, these two exclusive processes may provide us with independent phenomenological constraints to the color-singlet NRQCD LDMEs for the S-wave charmonia.

The remainder of this paper is organized as follows. In Sec. II, we briefly describe the strategy of resumming relativistic corrections in a quarkonium process. In Sec. III, we compute the cross section for $e^+e^- \to \eta_c + \gamma$, in which the QCD NLO and resummed relativistic corrections, and their interference are included within the standard NRQCD factorization approach. The corresponding cross section for $e^+e^- \to J/\psi + J/\psi$ is given in Sec. IV. In the case of $e^+e^- \to J/\psi + J/\psi$, that is dominated by the photon fragmentation, the result within the standard NRQCD approach gives negative cross section. As an alternative, we also employ the VMD approach to find an improved prediction. Finally, we conclude in Sec. V.

II. STRATEGY OF RESUMMING RELATIVISTIC CORRECTIONS

In this section, we list the NRQCD factorization formula for the cross sections of $e^+e^- \to \eta_c + \gamma$ and $e^+e^- \to J/\psi + J/\psi$, and summarize the strategy of resumming relativistic corrections.

A. NRQCD factorization formula

According to the NRQCD factorization formalism [1], the cross sections for the exclusive processes $e^+e^- \to \eta_c + \gamma$ and $e^+e^- \to J/\psi + J/\psi$ can be expressed as:

$$\sigma[e^+e^- \to \eta_c + \gamma] = \sum_n \frac{F_n}{m_c^5} \langle \mathcal{O}_n^{\eta_c} \rangle, \tag{1a}$$

$$\sigma[e^+e^- \to J/\psi + J/\psi] = \sum_{m,n} \frac{F_{m,n}}{m_c^8} \langle \mathcal{O}_m^{J/\psi} \rangle \langle \mathcal{O}_n^{J/\psi} \rangle, \tag{1b}$$

where $\langle \mathcal{O}_n^H \rangle$ is the NRQCD LDME for production of a quarkonium H from a $c\bar{c}_n$ pair with a spectroscopic state n, F_n and $F_{m,n}$ are dimensionless perturbative short-distance coefficients that are independent of the long-distance nature of H, and m_c is the charm-quark mass.

In general, the quantum number for $c\bar{c}_n$ does not have to be the same as that for the quarkonium H and the numerical importance of a $c\bar{c}_n$ channel relative to the color-singlet channel is classified in powers of v in the velocity-scaling rules of NRQCD. In the exclusive process (1), $c\bar{c}_n$ channels with the quantum number identical to that of H contribute dominantly. Thus the series (1) can be well approximated by the relativistic corrections and the index n can be understood as the power in v^2 relative to the LO color-singlet NRQCD LDME $\langle \mathcal{O}_0^H \rangle$. The expression (1) can further be simplified once we apply the vacuum-saturation approximation to express the production LDME in terms of the corresponding decay LDME $\langle \mathcal{O}_n \rangle_H$: $\langle \mathcal{O}_n^H \rangle \approx (2J+1)\langle \mathcal{O}_n \rangle_H$, where J is the total-angular-momentum quantum number of H. In the Coulomb gauge, the relative-order-v^{2n} decay LDMEs for $H = J/\psi$ and η_c are expressed as

$$\langle \mathcal{O}_n \rangle_{J/\psi} = \langle J/\psi(\lambda)|\psi^\dagger \left(-\tfrac{i}{2}\overleftrightarrow{\boldsymbol{D}}\right)^{2a} \boldsymbol{\sigma}\cdot\boldsymbol{\epsilon}^*(\lambda)\chi|0\rangle\langle 0|\chi^\dagger \left(-\tfrac{i}{2}\overleftrightarrow{\boldsymbol{D}}\right)^{2b} \boldsymbol{\sigma}\cdot\boldsymbol{\epsilon}(\lambda)\psi|J/\psi(\lambda)\rangle, \tag{2a}$$

$$\langle \mathcal{O}_n \rangle_{\eta_c} = \langle \eta_c|\psi^\dagger \left(-\tfrac{i}{2}\overleftrightarrow{\boldsymbol{D}}\right)^{2a} \chi|0\rangle\langle 0|\chi^\dagger \left(-\tfrac{i}{2}\overleftrightarrow{\boldsymbol{D}}\right)^{2b} \psi|\eta_c\rangle, \tag{2b}$$

where $n = a+b$,[1] $\psi^\dagger$ and χ are two-component Pauli spinor fields that create a heavy quark and a heavy antiquark, respectively, σ^i is a Pauli matrix, $\boldsymbol{D}$ is the spatial component of the covariant derivative, and λ and $\boldsymbol{\epsilon}(\lambda)$ are the helicity and polarization vector of J/ψ, respectively.[2] The state $|H\rangle$ is normalized nonrelativistically: $\langle H(\boldsymbol{P})|H(\boldsymbol{P}')\rangle = (2\pi)^3\delta^{(3)}(\boldsymbol{P}-\boldsymbol{P}')$.

[1] If $a \neq b$, the right side of Eq. (2) is understood to be the average with its Hermitian conjugate.

[2] In general, there are additional contributions that depend on chromoelectromagnetic field operators that

The LO color-singlet LDMEs are given by

$$\langle O_0\rangle_{J/\psi} = \left|\langle 0|\chi^\dagger \boldsymbol{\sigma}\cdot\boldsymbol{\epsilon}(\lambda)\psi|J/\psi(\lambda)\rangle\right|^2, \tag{3a}$$

$$\langle O_0\rangle_{\eta_c} = \left|\langle 0|\chi^\dagger\psi|\eta_c\rangle\right|^2. \tag{3b}$$

B. Resummation of relativistic corrections

The amplitude of an S-wave charmonium H produced associated with a particle a in an e^+e^- annihilation can be expressed as

$$\mathcal{A}[e^+e^- \to H + a] = \sum_{n=0}^{\infty}\left[\frac{1}{n!}\left(\frac{\partial}{\partial \boldsymbol{q}^2}\right)^n \mathcal{M}(\boldsymbol{q}^2)\right]\Bigg|_{\boldsymbol{q}^2=0} \langle \boldsymbol{q}^{2n}\rangle_H \langle \mathcal{O}_0\rangle_H^{1/2}, \tag{4}$$

where $\mathcal{M}(\boldsymbol{q}^2)$ is the corresponding parton-level amplitude with the standard normalization in the NRQCD factorization approach in which the angular dependence of half the relative momentum $\boldsymbol{q}$ of the c and $\bar{c}$ has been averaged in the $c\bar{c}$ rest frame. $\langle \boldsymbol{q}^{2n}\rangle_H$ is the ratio of the HO LDME of order v^{2n} relative to the LO one. For $H = J/\psi$,

$$\langle \boldsymbol{q}^{2n}\rangle_{J/\psi} = \frac{\langle 0|\chi^\dagger(-\frac{i}{2}\overleftrightarrow{\boldsymbol{D}})^{2n}\boldsymbol{\sigma}\cdot\boldsymbol{\epsilon}(\lambda)\psi|J/\psi(\lambda)\rangle}{\langle 0|\chi^\dagger\boldsymbol{\sigma}\cdot\boldsymbol{\epsilon}(\lambda)\psi|J/\psi(\lambda)\rangle}. \tag{5}$$

Eventually in the factorization formula (1), the long-distance factors in Eq. (4) are expressed in terms of the LDMEs in Eq. (2) that are, in principle, independent of the LO LDMEs $\langle O_0\rangle_H$ in Eq. (3). In Ref. [10], the Cornell potential model was used to express the ratio $\langle \boldsymbol{q}^{2n}\rangle_H$ in terms of $\langle \boldsymbol{q}^2\rangle_H$:

$$\langle \boldsymbol{q}^{2n}\rangle_H = \langle \boldsymbol{q}^2\rangle_H^n, \tag{6}$$

that we call the generalized Gremm-Kapustin relation[3]. The relation (6) neglects the gauge-field contribution to the covariant derivative in the Coulomb gauge and neglects the spin-flipping interactions so that $\langle \boldsymbol{q}^{2n}\rangle_{\eta_c} \approx \langle \boldsymbol{q}^{2n}\rangle_{J/\psi}$. Various applications and detailed descriptions of the uncertainties of applying the relation can be found in Refs. [10, 11, 15, 16, 27].

---

appear from relative order v^4. At the relative order v^4 such contribution can be expressed in terms of the operators of the same relative order in Eq. (2) [27, 28]. In this work, we neglect the gauge-field contribution in the Coulomb gauge and, therefore, the contributions of the chromoelectromagnetic field operators are also neglected.

[3] The original form of the Gremm-Kapustin relation is $\langle \boldsymbol{q}^2\rangle_H \approx (m_H - 2m_c)m_c$ [29], where m_H is the S-wave quarkonium mass.

The generalized Gremm-Kapustin relation (6) allows one to resum a class of relativistic corrections to all orders in v. The resultant amplitude is

$$\mathcal{A}[e^+e^- \to H + a] = \mathcal{M}(\langle \boldsymbol{q}^2 \rangle_H) \langle \mathcal{O}_0 \rangle_H^{1/2} \,. \tag{7}$$

It is straightforward to apply this resummation method to $e^+e^- \to \eta_c + \gamma$ and $e^+e^- \to J/\psi + J/\psi$.

C. The VMD approach

In Ref. [4], the importance of the photon-fragmentation contribution in the J/ψ production in e^+e^- annihilation was considered and the competition between the QED and QCD contributions was first observed. The dominance of the photon fragmentation in $e^+e^- \to J/\psi + J/\psi$ at the B factories was predicted in Refs. [20, 21, 23]. In spite of a suppression factor α^2/α_s^2 relative to the QCD subprocesses of other exclusive two-quarkonium production in e^+e^- annihilation, the photon-fragmentation contribution is largely enhanced by a kinematic factor $[\sqrt{s}/(2m_c)]^4$ that is associated with the fragmentation of a photon into a $c\bar{c}$ pair. The rate is further enhanced by a factor of $\log[\sqrt{s}/(2m_c)]$ originated from the collinear emission of a virtual photon in the forward region. Similar enhancement of the photon-fragmentation contribution was predicted in inclusive J/ψ production with sufficiently large transverse momentum p_T at hadron colliders [30, 31].

As is stated in Refs. [11, 23], the prediction of the photon-fragmentation contribution in $e^+e^- \to J/\psi + J/\psi$ can be improved by employing the VMD approach. We shall find later that after combining the QCD NLO and resummed relativistic corrections to $e^+e^- \to J/\psi + J/\psi$, the cross section becomes negative within the standard NRQCD factorization approach. As an alternative, we employ the VMD approach to cure this symptom.

If the photon-fragmentation dominance is valid, then one can neglect the non-fragmentation contributions that make a gauge-invariant subset. In that case, the amplitude is factorized into the product of $\mathcal{M}[e^+e^- \to \gamma^* + \gamma^*]$ and the $\gamma^* \to J/\psi$ fragmentation factor that involves the local electromagnetic current

$$J^\mu(x) = e_c e \bar{c}(x) \gamma^\mu c(x) \tag{8}$$

for a free $c\bar{c}$ pair created at a fixed point x. Here, e is the electron charge and e_c is the fractional electric charge of the charm quark. In VMD, the long-distance factor for the transition of the pair to J/ψ is expressed as

$$\langle J/\psi(\lambda)|J^\mu(x=0)|0\rangle = g_{J/\psi\gamma}\epsilon^{*\mu}(\lambda), \tag{9}$$

where $g_{J/\psi\gamma}$ is the effective J/ψ-photon coupling. Applying this vertex to $J/\psi \to e^+e^-$, one can determine the coupling $g_{J/\psi\gamma}$ [11, 23] as

$$g_{J/\psi\gamma} = \left(\frac{3m_{J/\psi}^3}{4\pi\alpha^2}\Gamma[J/\psi \to e^+e^-]\right)^{\frac{1}{2}}. \tag{10}$$

If we can neglect the virtual-gluon corrections to the photon-fragmentation process that connect the two $c\bar{c}$ lines, then the vertex (9) collects the QCD HO and relativistic corrections effectively. We can make an educated guess that a virtual-gluon correction, that appears from relative order α_s^2, is negligible because the contribution is suppressed by α_s^2 relative to the LO and the kinematic enhancement is reduced due to the stronger virtualites of the internal lines. Because we use the measured values for the decay rate $\Gamma[J/\psi \to e^+e^-]$ and the J/ψ mass $m_{J/\psi}$, in evaluating the effective coupling (10), large theoretical uncertainties can be replaced with tiny experimental errors. We take the scale $m_{J/\psi}$, which is the momentum scale at the vertex, in computing the fine structure constant α in Eq. (10).

D. Interference

In a previous analysis in Ref. [11] on $e^+e^- \to J/\psi+\eta_c$, the authors found that both QCD NLO and resummed relativistic corrections to the cross section were significant. It was also reported that the interference between the two corrections was about 26 % of the LO cross section. Thus we expect that the interference term may also be important in other processes that have large QCD and relativistic corrections. In addition to this interference there is another order-$\alpha_s v^2$ correction that can be computed directly from the order-α_s diagrams by keeping the v dependence. Such order-$\alpha_s v^2$ corrections were computed for $J/\psi \to \ell^+\ell^-$ [16], $B_c \to \ell\nu$ [32], $\eta_c \to \gamma\gamma$ and LH [18, 33], $e^+e^- \to J/\psi + \eta_c$ [14], h_c, h_b and $\eta_b \to$ LH [34], and $J/\psi \to 3\gamma$ [35]. Many of the corrections are tiny, for example, at most 0.3 % in $J/\psi \to \ell^+\ell^-$ [16]. Some exceptions are $h_c \to$ LH [34] and $J/\psi \to 3\gamma$ [35], which have significant order-$\alpha_s v^2$ corrections.

In this work, we improve the theoretical prediction for the production rates of $e^+e^- \to \eta_c + \gamma$ and $e^+e^- \to J/\psi + J/\psi$ by including the order-α_s and order-v^∞ corrections, and

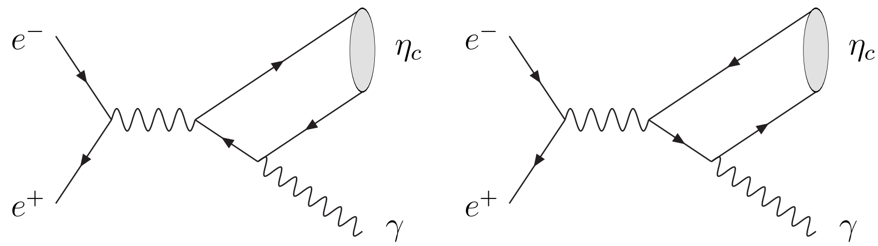

FIG. 1: Feynman diagrams for $e^+e^- \to \eta_c + \gamma$ at LO in α_s.

their interference.[4] The computation of the pure order-$\alpha_s v^2$ contribution, that is out of the scope of this work, is not included. The missing contribution is of the same order as the interference term that may bring in theoretical errors. Equation (42) of Ref. [11] includes the three contributions listed above to the total cross section σ_{tot}:

$$\sigma_{\text{tot}} = \sigma_{v^\infty} + \sqrt{\sigma_{v^\infty}} \frac{\sigma_{\text{NLO}} - \sigma_0}{\sqrt{\sigma_0}} = \sigma_{v^\infty} + \sqrt{\sigma_{v^\infty} \sigma_0} \, (K_{\alpha_s} - 1) \, , \tag{11}$$

where σ_0, σ_{v^∞}, and σ_{NLO} are the cross sections at the LO, order v^∞, and order α_s, respectively, and $K_{\alpha_s} \equiv \sigma_{\text{NLO}}/\sigma_0$. The approximation for the interference term in Eq. (11) is constructed under the assumption that K_{α_s} and v^∞ corrections are independent of the polarization λ of H. Violation of this assumption may cause additional theoretical errors.

III. $e^+e^- \to \eta_c + \gamma$

In this section, we compute the cross section for $e^+e^- \to \eta_c + \gamma$ at $\sqrt{s} = 10.58\,\text{GeV}$ by employing the strategies given in Sec. II. In e^+e^- annihilation, this process proceeds with the parton process $e^+e^- \to c\bar{c}({}^1S_0^{[1]}) + \gamma$, where $c\bar{c}({}^1S_0^{[1]})$ is the color-singlet spin-singlet S-wave $c\bar{c}$ pair. Because both QED and QCD have the charge-conjugation symmetry and η_c is an even charge-conjugation eigenstate, the process factors into the leptonic part $e^+e^- \to \gamma^*$ and the hadronic part $\gamma^* \to c\bar{c}({}^1S_0^{[1]}) + \gamma$. At the LO in α_s, two Feynman diagrams contribute to this process as shown in Fig. 1.

[4] In the remainder of this paper, we use the notation v^∞ in order to indicate that a quantity is resummed to all orders in v.

A. Amplitude

In order to construct the amplitude for $e^+e^- \to c\bar{c}({}^1S_0^{[1]}) + \gamma$, we first write the amplitude $\mathcal{M}$ for the process $e^+(k_2)e^-(k_1) \to c(p)\bar{c}(\bar{p}) + \gamma(P_\gamma)$ as

$$\mathcal{M} = L^\mu \mathcal{H}_\mu, \tag{12}$$

where the momentum of each particle is written in the parentheses following each particle identity. Here, the leptonic current L^μ is defined by

$$L^\mu = \frac{e}{s}\bar{v}(k_2)\gamma^\mu u(k_1). \tag{13}$$

The hadronic current $\mathcal{H}_\mu$ is given by $\mathcal{H}_\mu = \bar{u}(c)\mathcal{C}_\mu v(\bar{c})$ with $\mathcal{C}_\mu = \mathcal{C}_{\mu\nu}\epsilon^{*\nu}$, ϵ is the polarization vector of the photon, and the Dirac and color indices of $\mathcal{C}_{\mu\nu}$ are suppressed. The momenta p and $\bar{p}$ for the on-shell c and $\bar{c}$, respectively, are linear combinations of the quarkonium momentum P and half the relative momentum q:

$$p = \tfrac{1}{2}P + q, \tag{14a}$$

$$\bar{p} = \tfrac{1}{2}P - q. \tag{14b}$$

At the $c\bar{c}$ rest frame, $P = [2E(q), \mathbf{0}]$, $q = (0, \boldsymbol{q})$, $p = [E(q), \boldsymbol{q}]$, and $\bar{p} = [E(q), -\boldsymbol{q}]$, where $E(q) = \sqrt{m_c^2 + \boldsymbol{q}^2}$.

The color-singlet spin-singlet contribution can be projected out from $\mathcal{H}_\mu$ by taking the trace after multiplying the projectors for the spin-singlet $[\Pi_1(p,\bar{p})]$ and the color-singlet (π_1) state. The corresponding projectors are defined by

$$\Pi_1(p,\bar{p}) = \frac{1}{4\sqrt{2}E(q)[E(q)+m_c]}(\not{\bar{p}} - m_c)\gamma^5[\not{P} + 2E(q)](\not{p} + m_c), \tag{15a}$$

$$\pi_1 = \frac{1}{\sqrt{N_c}}\mathbb{1}, \tag{15b}$$

where $N_c = 3$ is the number of colors and $\mathbb{1}$ is the unit color matrix. The spin projector (15a) contains the q dependence to all orders in v [28]. Then the $c\bar{c}({}^1S_0^{[1]})$ contribution $\mathcal{H}_\mu[c\bar{c}({}^1S_0^{[1]})]$ to the hadronic current is finally obtained by averaging over the directions of $\boldsymbol{q}$ in the $c\bar{c}$ rest frame:

$$\mathcal{H}_\mu[c\bar{c}({}^1S_0^{[1]})] = \int \frac{d\Omega_{\boldsymbol{q}}}{4\pi}\,\mathrm{Tr}\left[\mathcal{H}_\mu \Pi_1(p,\bar{p}) \otimes \pi_1\right], \tag{16}$$

where $\Omega_{\boldsymbol{q}}$ is the solid angle of $\boldsymbol{q}$ and the trace is over the color and spinor indices. Now the complete q dependence in Eq. (16) is a function of $\boldsymbol{q}^2$. Carrying out the standard perturbative matching of the full-QCD amplitude for the hadronic current to the NRQCD counterpart and employing the resummation strategy stated in Sec. II B, we obtain the amplitude for $e^+e^- \to \eta_c + \gamma$ as

$$\mathcal{A}[e^+e^- \to \eta_c + \gamma] = L_\mu \left. \left[\frac{1}{2N_c\sqrt{E(q)}} \mathcal{H}_\mu[c\bar{c}(^1S_0^{[1]})] \right] \right|_{\boldsymbol{q}^2=\langle \boldsymbol{q}^2\rangle_{\eta_c}} \langle O_0 \rangle_{\eta_c}^{1/2}. \tag{17}$$

B. Kinematics

Because of the average over the angle for $\boldsymbol{q}$ that is required to project out the S-wave state, additional consideration of the $\boldsymbol{q}$ dependence in the $c\bar{c}$ amplitude is needed. As is stated in Ref. [11], it is convenient to choose the e^+e^- CM frame in which the final momenta are along the z-axis. In this CM frame, the momenta for e^-, e^+, η_c, and γ are given by

$$k_1 = \frac{\sqrt{s}}{2}(1, \sin\theta, 0, \cos\theta), \tag{18a}$$

$$k_2 = \frac{\sqrt{s}}{2}(1, -\sin\theta, 0, -\cos\theta), \tag{18b}$$

$$P = (E_P, 0, 0, P_{\rm CM}), \tag{18c}$$

$$P_\gamma = (P_{\rm CM}, 0, 0, -P_{\rm CM}), \tag{18d}$$

where θ is the scattering angle, $E_P = [s + 4E^2(q)]/(2\sqrt{s})$, and $P_{\rm CM} = [s - 4E^2(q)]/(2\sqrt{s})$. The explicit form of q in this CM frame is given by

$$q = |\boldsymbol{q}| (\gamma_q\beta_q\cos\theta_q, \sin\theta_q\cos\phi_q, \sin\theta_q\sin\phi_q, \gamma_q\cos\theta_q), \tag{19}$$

where $|\boldsymbol{q}| \equiv \sqrt{-q^2}$ and the two factors $\gamma_q = E_P/[2E(q)]$ and $\beta_q = P_{\rm CM}/E_P$ involve the boost from the $c\bar{c}$ rest frame to this e^+e^- CM frame. θ_q and ϕ_q are the polar and azimuthal angles, respectively, of q^* that is the explicit form of q in the $c\bar{c}$ rest frame:

$$q^* = |\boldsymbol{q}| (0, \sin\theta_q\cos\phi_q, \sin\theta_q\sin\phi_q, \cos\theta_q). \tag{20}$$

C. Cross section

Summing over the final spins and averaging over the initial spins of the absolute square of the amplitude $\mathcal{A}[e^+e^- \to \eta_c + \gamma]$ in Eq. (17), we obtain the spin-averaged squared amplitude

TABLE I: The cross sections σ_0, σ_{v^∞}, and $\sigma_{\rm tot}$ for $e^+e^- \to \eta_c + \gamma$ in units of fb at the scales $\mu = m_c$ and $2m_c$ with the input parameters m_c, $\langle O_0\rangle_{\eta_c}$, $\langle \boldsymbol{q}^2\rangle_{\eta_c}$, in units of GeV, GeV^3, and GeV^2, respectively. The errors of the cross sections reflect the uncertainties of the NRQCD LDMEs only.

m_c	$\langle O_0\rangle_{\eta_c}$	$\langle \boldsymbol{q}^2\rangle_{\eta_c}$	σ_0	σ_{v^∞}	$\sigma_{\rm tot}$	
					$\mu = m_c$	$\mu = 2m_c$
1.4	$0.437^{+0.111}_{-0.105}$	0.442 ± 0.143	$83.2^{+21.1}_{-20.0}$	$68.9^{+18.0}_{-17.0}$	$51.5^{+13.6}_{-12.8}$	$55.3^{+14.5}_{-13.7}$

$\overline{|\mathcal{A}[e^+e^- \to \eta_c + \gamma]|^2}$. Dividing it by the flux factor $2s$, and integrating over the phase space, we find the cross section.

In order to evaluate the cross section for $e^+e^- \to \eta_c + \gamma$ we first choose the numerical values for the input parameters. We choose $\alpha = 1/131$ that is the running coupling constant evaluated at scale $\mu = \sqrt{s}$ [15, 24]. As is shown in the first three columns in Table I, we choose m_c, $\langle O_0\rangle_{\eta_c}$, and $\langle \boldsymbol{q}^2\rangle_{\eta_c}$ from Refs. [15, 24]. The LO cross section σ_0 is consistent with previous results in Refs. [24, 25] [5]. We recall that σ_{v^∞} is the order-α_s^0 contribution in which order-v^∞ corrections are resummed. The order-v^∞ correction σ_{v^∞} is about $-17\,\%$ of σ_0. We have estimated the order-v^2 corrections from our resummed formula by taking the partial derivative with respect to $\langle \boldsymbol{q}^2\rangle_{\eta_c}$ numerically. Our result is $-75.6\,\langle v^2\rangle_{\eta_c}$, which is in good agreement with the value $-75.5\,\langle v^2\rangle_{\eta_c}$ obtained from the fixed-order calculation in Ref. [25]. We define $K_{v^2} = \sigma_{v^2}/\sigma_0$ and $K_{v^\infty} = \sigma_{v^\infty}/\sigma_0$, where σ_{v^2} is the cross section that includes the corrections of order $\alpha_s^0 v^2$. The results are $K_{v^2} = 0.80$ and $K_{v^\infty} = 0.83$ which imply that the contributions of order v^4 or higher enhance the cross section by about $4\,\%$. This is a good signal that the v expansion converges very well.

The factor K_{α_s} defined by $\sigma_{\rm NLO}/\sigma_0$ is 0.77 for $\mu = m_c$ and 0.82 for $\mu = 2m_c$, respectively [25]. Taking into account both the NLO corrections in α_s and the relativistic corrections, and the interference between them, we find the total cross section $\sigma_{\rm tot} = 51.5^{+13.6}_{-12.8}$ fb for $\mu = m_c$ and $\sigma_{\rm tot} = 55.3^{+14.5}_{-13.7}$ fb for $\mu = 2m_c$, respectively. For a luminosity of 1 (10) ab^{-1} at B (super B) factories, the expected number of events is about 5×10^4 (5×10^5). Since the branching fraction of the η_c decay into two photons is $(1.78 \pm 0.16) \times 10^{-4}$ [36], $e^+e^- \to \eta_c + \gamma$ followed by $\eta_c \to \gamma\gamma$ might be observed at Belle II or super B factory, but the events might not be

[5] The errors of the cross sections reflect the uncertainties of the NRQCD LDMEs only.

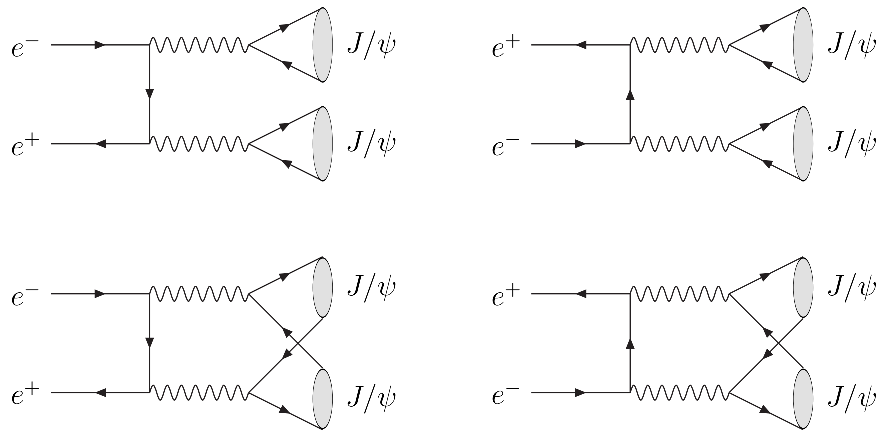

FIG. 2: Feynman diagrams for $e^+e^- \to J/\psi + J/\psi$.

triggered because no charged particles exist in the detector. Instead, the $\eta_c \to K\bar{K}\pi$ mode, whose branching fraction is $(7.2 \pm 0.6)\,\%$ [36], may be useful to observe the $e^+e^- \to \eta_c + \gamma$ events. The analysis of the photon energy spectrum in $e^+e^- \to K\bar{K}\pi + \gamma$ will be useful to detect this channel [24].

IV. $e^+e^- \to J/\psi + J/\psi$

In this section, we consider the $e^+e^- \to J/\psi + J/\psi$ process at $\sqrt{s} = 10.58$ GeV. This process proceeds through e^+e^- annihilation into two virtual photons because the charge-conjugation parity of J/ψ is -1. At the LO in α_s, there are four Feynman diagrams as shown in Fig. 2. The first two diagrams are called the photon-fragmentation diagrams, where each virtual photon evolves into a J/ψ. The other two diagrams in the second row are called the nonfragmentation diagrams, where two virtual photons evolve into two J/ψ mesons. The invariant mass of the virtual photon in the photon-fragmentation diagrams is fixed as $m_{J/\psi}$, but the typical momentum scale of the virtual photons in the nonfragmentation diagrams is of order $\sqrt{s}/2$.

A. Amplitude of $e^+e^- \to c\bar{c}(^3S_1^{[1]}) + c\bar{c}(^3S_1^{[1]})$

In order to calculate the relativistic corrections to the double J/ψ production in e^+e^- collisions, we first construct the amplitude for the production of two color-singlet spin-triplet S-wave $c\bar{c}(^3S_1^{[1]})$ pairs in e^+e^- collisions. The amplitude for $e^+(k_2)e^-(k_1) \to c(p_1)\bar{c}(\bar{p}_1) +$

$c(p_2)\bar{c}(\bar{p}_2)$ can be written as

$$\mathcal{M} = \sum_{j=1}^{4} L^{j\mu\nu} \mathcal{A}^{j}_{\mu\nu}[c_1\bar{c}_1 + c_2\bar{c}_2], \tag{21}$$

where $L^{j\mu\nu}$ and $\mathcal{A}^{j}_{\mu\nu}$ are the leptonic and hadronic tensors for each diagram. Eventually, each $c_i(p_i)\bar{c}_i(\bar{p}_i)$ pair evolves into a J/ψ meson.

The amplitude $\mathcal{A}^{j}_{\mu\nu}[P_1, q_1, \lambda_1; P_2, q_2, \lambda_2]$ for the production of two $c\bar{c}(^3S_1^{[1]})$ pairs from the two virtual photons can be obtained by projecting the amplitude $\mathcal{A}^{j}_{\mu\nu}[c_1\bar{c}_1 + c_2\bar{c}_2]$ into the color-singlet spin-triplet channel, where P_i, q_i, and λ_i are the four-momentum of the $c_i\bar{c}_i$ pair, half the relative momentum of c_i and $\bar{c}_i$, and the polarization vector of the $c_i\bar{c}_i$ pair, respectively, with the following relations:

$$p_i = \frac{P_i}{2} + q_i, \tag{22a}$$

$$\bar{p}_i = \frac{P_i}{2} - q_i. \tag{22b}$$

The spin-triplet projector for $c_i\bar{c}_i$ pair, which is valid for v^∞ corrections, is given by [28]

$$\Pi_3^i(p_i, \bar{p}_i, \lambda_i) = -\frac{1}{4\sqrt{2}E(q_i)[E(q_i)+m_c]}(\not{\bar{p}}_i - m_c)\,\not{\epsilon}_i^*(\lambda_i)[\not{P}_i + 2E(q_i)](\not{p}_i + m_c), \tag{23}$$

where $\epsilon_i(\lambda_i)$ is the polarization vector of the $c_i\bar{c}_i$ pair with the polarization λ_i and $E(q_i)$ is the energy of the charm quark or antiquark in the $c_i\bar{c}_i$ rest frame. We note that the $c_i\bar{c}_i$ pair in $\mathcal{A}^{j}_{\mu\nu}[P_1, q_1, \lambda_1; P_2, q_2, \lambda_2]$ is not a pure S-wave state.

The S-wave contribution can be extracted by averaging the amplitude over the polar and azimuthal angles of $\boldsymbol{q}_i$, which is the spatial vector of q_i, in the $c_i\bar{c}_i$ rest frame:

$$\mathcal{A}^{j}_{\mu\nu}[(c_1\bar{c}_1)(^3S_1^{[1]}) + (c_2\bar{c}_2)(^3S_1^{[1]})] \equiv \int \frac{d\Omega_1 d\Omega_2}{(4\pi)^2}\mathcal{A}^{j}_{\mu\nu}[P_1, q_1, \lambda_1; P_2, q_2, \lambda_2]. \tag{24}$$

Now the q_i dependence of the quantity in Eq. (24) is a function of $\boldsymbol{q}_1^2$ and $\boldsymbol{q}_2^2$. Here, Ω_i is the solid angle of $\boldsymbol{q}_i$ in the $c_i\bar{c}_i$ rest frame. As we did in the previous section, we do not find the short-distance coefficients by expanding Eq. (24) in terms of $\boldsymbol{q}_i^2$. Instead, we employ the formula (7) to obtain the amplitude in which relativistic corrections are resummed:

$$\begin{aligned}\mathcal{A}^{j}_{\mu\nu}[J/\psi + J/\psi] \;=\; & \left[\frac{1}{4N_c^2\sqrt{E(q_1)E(q_2)}}\mathcal{A}^{j}_{\mu\nu}[(c_1\bar{c}_1)(^3S_1^{[1]}) + (c_2\bar{c}_2)(^3S_1^{[1]})]\right]\Bigg|_{\boldsymbol{q}_1^2=\boldsymbol{q}_2^2=\langle \boldsymbol{q}^2\rangle_{J/\psi}} \\ & \times\langle O_0\rangle^{1/2}_{J/\psi}\langle O_0\rangle^{1/2}_{J/\psi}.\end{aligned} \tag{25}$$

B. Kinematics

We first compute the cross section for $e^+e^- \to J/\psi + J/\psi$ within the standard NRQCD factorization approach. Then, as an alternative, we employ the VMD approach for the photon-fragmentation diagrams while keeping the standard NRQCD factorization approach for the nonfragmentation diagrams as in Ref. [23]. Note that we use the expression P_i for the $c_i\bar{c}_i$ four-momentum depending on the approach: In the NRQCD approach, we set $P_i^2 = [2E(q_i)]^2$, while we set $P_i^2 = m_{J/\psi}^2$ in the VMD approach.

1. *Kinematics for the NRQCD factorization approach*

In the calculation within the standard NRQCD factorization approach, the four-momenta of $e^\pm$ and $c_i\bar{c}_i$ pairs at the e^+e^- CM frame are given by

$$k_1 = \frac{\sqrt{s}}{2}(1, \sin\theta, 0, \cos\theta), \tag{26a}$$

$$k_2 = \frac{\sqrt{s}}{2}(1, -\sin\theta, 0, -\cos\theta), \tag{26b}$$

$$P_1 = (E_1, 0, 0, |\boldsymbol{P}|), \tag{26c}$$

$$P_2 = (E_2, 0, 0, -|\boldsymbol{P}|), \tag{26d}$$

where $E_1 = [s + 4E(q_1)^2 - 4E(q_2)^2]/(2\sqrt{s})$, $E_2 = [s - 4E(q_1)^2 + 4E(q_2)^2]/(2\sqrt{s})$, and $|\boldsymbol{P}| = \lambda^{1/2}(s, 4E(q_1)^2, 4E(q_2)^2)/(2\sqrt{s})$ with $\lambda(a,b,c) = a^2 + b^2 + c^2 - 2ab - 2bc - 2ca$. The polarization vectors of the $c_i\bar{c}_i$ pairs are given by

$$\epsilon_1^*(0) = \frac{1}{\sqrt{E_1^2 - |\boldsymbol{P}|^2}}(|\boldsymbol{P}|, 0, 0, E_1), \tag{27a}$$

$$\epsilon_2^*(0) = \frac{1}{\sqrt{E_2^2 - |\boldsymbol{P}|^2}}(-|\boldsymbol{P}|, 0, 0, E_2), \tag{27b}$$

$$\epsilon_1^*(\pm) = -\epsilon_2^*(\mp) = \mp\frac{1}{\sqrt{2}}(0, 1, \mp i, 0). \tag{27c}$$

In each rest frame of the $c_i\bar{c}_i$ pair, half the relative momentum q_i^* is given by

$$q_i^* = |\boldsymbol{q}_i|\,(0, \sin\theta_i^*\cos\phi_i^*, \sin\theta_i^*\sin\phi_i^*, \cos\theta_i^*), \tag{28}$$

where θ_i^* and ϕ_i^* are the polar and azimuthal angles of $\boldsymbol{q}_i^*$, respectively, and $|\boldsymbol{q}_i|$ is the magnitude of $\boldsymbol{q}_i^*$ in the $c_i\bar{c}_i$ rest frame. Boosting Eq. (28) from the $c_i\bar{c}_i$ rest frame to the

e^+e^- CM frame, one obtains

$$q_1 = |\boldsymbol{q}_1| \left(\gamma_1\beta_1 \cos\theta_1^*, \sin\theta_1^* \cos\phi_1^*, \sin\theta_1^* \sin\phi_1^*, \gamma_1 \cos\theta_1^*\right), \tag{29a}$$

$$q_2 = |\boldsymbol{q}_2| \left(\gamma_2\beta_2 \cos\theta_2^*, \sin\theta_2^* \cos\phi_2^*, \sin\theta_2^* \sin\phi_2^*, \gamma_2 \cos\theta_2^*\right), \tag{29b}$$

where $\gamma_i = E_i/[2E(q_i)]$, $\beta_1 = |\boldsymbol{P}|/E_1$, and $\beta_2 = -|\boldsymbol{P}|/E_2$.

2. *Kinematics for the VMD approach*

In the calculation within the VMD approach, the four-momenta and polarization vectors for the $c_i\bar{c}_i$ pairs at the e^+e^- CM frame are given by

$$P_1^{\text{fr}} = (E_1^{\text{fr}}, 0, 0, |\boldsymbol{P}^{\text{fr}}|), \tag{30a}$$

$$P_2^{\text{fr}} = (E_2^{\text{fr}}, 0, 0, -|\boldsymbol{P}^{\text{fr}}|), \tag{30b}$$

$$\epsilon_1^{\text{fr}*}(0) = \frac{1}{\sqrt{E_1^{\text{fr}2} - |\boldsymbol{P}^{\text{fr}}|^2}}(|\boldsymbol{P}^{\text{fr}}|, 0, 0, E_1^{\text{fr}}), \tag{30c}$$

$$\epsilon_2^{\text{fr}*}(0) = \frac{1}{\sqrt{E_2^{\text{fr}2} - |\boldsymbol{P}^{\text{fr}}|^2}}(-|\boldsymbol{P}^{\text{fr}}|, 0, 0, E_2^{\text{fr}}), \tag{30d}$$

$$\epsilon_1^{\text{fr}*}(\pm) = -\epsilon_2^{\text{fr}*}(\mp) = \mp\frac{1}{\sqrt{2}}(0, 1, \mp i, 0), \tag{30e}$$

where $E_1^{\text{fr}} = E_2^{\text{fr}} = \sqrt{s}/2$ and $|\boldsymbol{P}^{\text{fr}}| = (s - 4m_{J/\psi}^2)^{1/2}/2$. Here, we use the superscript fr to denote that the variables are for the VMD approach. The four-momenta for the $e^\pm$ are the same as those in Eqs. (26a) and (26b): $k_i^{\text{fr}} = k_i$. Because the photon-J/ψ vertex (10) already contains the relativistic corrections to the photon-fragmentation diagrams, we do not take the average over the angles of $\boldsymbol{q}_1$ and $\boldsymbol{q}_2$.

C. Numerical results for NRQCD prediction

Applying the method described in Sec. IV B 1, we carry out the numerical computation of the cross section $\sigma[e^+e^- \to J/\psi + J/\psi]$ at the B factories within the standard NRQCD factorization approach. We take $\alpha = 1/131$ and vary the charm-quark mass as $m_c = 1.4$ and 1.5 GeV. The results are summarized in Table II depending on the input parameters. The LO NRQCD LDME $\langle O_0 \rangle_{J/\psi}$ and the ratio $\langle \boldsymbol{q}^2 \rangle_{J/\psi}$ are listed on the second and third columns of Table II, respectively. The values for $\langle O_0 \rangle_{J/\psi}$ and $\langle \boldsymbol{q}^2 \rangle_{J/\psi}$ at $m_c = 1.4$ GeV

TABLE II: The cross sections σ_0, σ_{v^∞}, and $\sigma_{\rm tot}$ for $e^+e^- \to J/\psi + J/\psi$ within the standard NRQCD factorization approach in units of fb at the scales $\mu = m_c$, $2m_c$, and $\sqrt{s}/2$ with the input parameters m_c, $\langle O_0\rangle_{J/\psi}$, $\langle \boldsymbol{q}^2\rangle_{J/\psi}$, in units of GeV, GeV^3, and GeV^2, respectively. The errors of the cross sections reflect the uncertainties of the NRQCD LDMEs only.

m_c	$\langle O_0\rangle_{J/\psi}$	$\langle \boldsymbol{q}^2\rangle_{J/\psi}$	σ_0	σ_{v^∞}	$\sigma_{\rm tot}$		
					$\mu = m_c$	$\mu = 2m_c$	$\mu = \sqrt{s}/2$
1.4	$0.440^{+0.067}_{-0.055}$	0.441 ± 0.140	$13.39^{+2.88}_{-2.37}$	$5.56^{+1.63}_{-1.35}$	$-12.74^{+2.51}_{-2.90}$	$-2.58^{+0.56}_{-0.60}$	$-0.89^{+0.51}_{-0.42}$
1.5	$0.436^{+0.065}_{-0.054}$	0.442 ± 0.140	$8.09^{+1.70}_{-1.42}$	$3.66^{+1.02}_{-0.85}$	$-6.96^{+1.34}_{-1.57}$	-1.36 ± 0.33	$-0.43^{+0.31}_{-0.25}$

are taken from Ref. [15]. The values at $m_c = 1.5$ GeV are obtained by applying the same method described in Ref. [15].

The result for the LO cross section σ_0 is listed on the third column of Table II. Our NRQCD prediction for σ_0 is greater than a previous result $\sigma_0 = 6.65 \pm 3.02$ fb in Ref. [20]. This is mainly because our value for $\langle O_0\rangle_{J/\psi}$ is greater than that (0.335 ± 0.024 GeV^3) of Ref. [20]. Our short-distance coefficient at LO in α_s agrees with those in Refs. [20, 22] and the numerical results also agree once we use the same numerical value for the LDME.

The cross section σ_{v^∞} in which the relativistic corrections are resummed to all orders in v is listed on the fourth column of Table II. The resummed result σ_{v^∞} is significantly smaller than the LO prediction σ_0 leading to $K_{v^\infty} = 0.42$ (0.45) at $m_c = 1.4$ (1.5) GeV. As we have mentioned, we can extract the order-v^2 relativistic corrections from the resummed formula by varying $\langle \boldsymbol{q}^2\rangle_{J/\psi}$ for each J/ψ numerically. The correction is $-28.4\,\langle v^2\rangle_{J/\psi}\,$fb ($-17.4\,\langle v^2\rangle_{J/\psi}\,$fb) at $m_c = 1.4$ (1.5) GeV for each J/ψ, where $\langle v^2\rangle_{J/\psi} \equiv \langle \boldsymbol{q}^2\rangle_{J/\psi}/m_c^2$. Taking into account the fact that there are two J/ψ mesons, we find that $K_{v^2} = 0.05$ (0.15) at $m_c =$ 1.4 (1.5) GeV. While the order-v^2 corrections are large negative, the relativistic corrections of order v^4 or higher significantly enhance the cross section.

The authors of Ref. [22] computed the cross section $\sigma_{\rm NLO}$ for $e^+e^- \to J/\psi + J/\psi$ at NLO in α_s, which has a strong dependence on m_c and the renormalization scale μ. According to the results, the QCD NLO corrections are large negative, leading to negative cross sections at $\mu = m_c$ for both $m_c = 1.4$ and 1.5 GeV. We can extract the factor $K_{\alpha_s} \equiv \sigma_{\rm NLO}/\sigma_0$ from the results in Table I of Ref. [22]: At $m_c = 1.4$ (1.5) GeV, $K_{\alpha_s} = -0.367$ (-0.314), 0.057 (0.077), and 0.253 (0.248) for $\mu = m_c$, $2m_c$, and $\sqrt{s}/2$, respectively.

Here, we notice that both the QCD NLO and order-v^2 relativistic corrections are large negative and significantly reduce the cross section for $e^+e^- \to J/\psi + J/\psi$. Thus, the interference between them must be large positive. In addition, the relativistic corrections of order v^4 or higher is large positive. Therefore, we expect that the interference contribution can be significant.

A rigorous computation of the interference contribution requires the information of the factor K_{α_s} for each polarization of two J/ψ mesons, which is not available yet. Therefore, we ignore the dependence on the J/ψ polarization and use the formula (11) for $\sigma_{\rm tot}$ to include the QCD NLO corrections, relativistic corrections, and their interference. Our results for $\sigma_{\rm tot}$ depending on the input parameters are given on the last three columns in Table II.[6] Every entry for $\sigma_{\rm tot}$ is negative, which is unphysical. We expect that one can resolve this problem only after including the corrections of orders α_s^2, $\alpha_s v^2$, or higher.

D. Numerical results with the VMD approach

In this section, we provide the numerical results for the cross section for $e^+e^- \to J/\psi + J/\psi$ in which the photon-fragmentation contribution is computed with the VMD approach. According to the NRQCD predictions in Refs. [20, 21], the nonfragmentation contribution to $e^+e^- \to J/\psi + J/\psi$ cross section is $0.9\,\%$, and the interference between the photon-fragmentation and nonfragmentation contributions is $-15.4\,\%$. This reveals that the photon-fragmentation contribution dominates in the process. In that limit, the VMD approach provides a good approximation for the photon-J/ψ vertex in the photon-fragmentation diagrams. The coupling in Eq. (10) collects both the QCD NLO and relativistic corrections to the photon-J/ψ vertex effectively and, therefore, the theoretical uncertainties can be greatly reduced [11]. Note that we cannot employ this method to compute the nonfragmentation diagrams and we apply the conventional NRQCD approach that is described in the previous section. This hybrid strategy can be justified because each contribution makes a separate gauge-invariant subset.

In estimating the coupling $g_{J/\psi\gamma}$ in Eq. (10), we take $\Gamma[J/\psi \to e^+e^-] = (5.55 \pm 0.14 \pm 0.02)$ keV [36] and $\alpha(\mu = m_{J/\psi}) = 1/132.6$, where the scale μ corresponds to the momentum

[6] At $\mu = m_c$, K_{α_s} is negative and, therefore, Eq. (11) is inapplicable to computing $\sigma_{\rm tot}$. In this case, we take $\sigma_{\rm tot} = \sigma_{v^\infty} + (K_{\alpha_s} - 1)\sigma_0$.

TABLE III: The cross sections $\sigma_0^{\rm fr}$, $\sigma_{v^\infty}^{\rm fr}$, and $\sigma_{\rm tot}^{\rm fr}$ for $e^+e^- \to J/\psi + J/\psi$ in units of fb, in which the photon-fragmentation contribution is computed with the VMD approach when $g_{J/\psi\gamma} = 0.832 \pm 0.010$ GeV^2. The description on the input parameters is the same as that in Table II.

m_c	$\langle O_0\rangle_{J/\psi}$	$\langle \boldsymbol{q}^2\rangle_{J/\psi}$	$\sigma_0^{\rm fr}$	$\sigma_{v^\infty}^{\rm fr}$	$\sigma_{\rm tot}^{\rm fr}$		
					$\mu = m_c$	$\mu = 2m_c$	$\mu = \sqrt{s}/2$
1.4	$0.440^{+0.067}_{-0.055}$	0.441 ± 0.140	1.81 ± 0.13	1.80 ± 0.13	$1.05^{+0.22}_{-0.25}$	$1.32^{+0.18}_{-0.20}$	$1.39^{+0.17}_{-0.19}$
1.5	$0.436^{+0.065}_{-0.054}$	0.442 ± 0.140	1.85 ± 0.13	1.84 ± 0.13	1.35 ± 0.20	$1.49^{+0.17}_{-0.18}$	1.56 ± 0.16

transfer at the vertex. In other vertices, we take $\alpha = 1/131$. The resultant numerical value is $g_{J/\psi\gamma} = 0.832 \pm 0.010$ GeV^2.

Our results for the cross sections $\sigma_0^{\rm fr}$, $\sigma_{v^\infty}^{\rm fr}$, and $\sigma_{\rm tot}^{\rm fr}$ are listed in Table III. Here, the superscript fr indicates that the photon-fragmentation contribution is computed with the VMD approach while the nonfragmentation diagrams are computed in the conventional NRQCD factorization approach. The description on the input parameters is the same as that in Table II. The uncertainties of the cross sections are dominated by the experimental errors in $\Gamma[J/\psi \to e^+e^-]$ through $g_{J/\psi\gamma}$. The LO cross sections $\sigma_0^{\rm fr}$ at $m_c = 1.4$ and 1.5 GeV agree with a previous result 1.69 ± 0.35 fb in Ref. [23] within errors. Sources of this small difference are as follows: While we use $2E_i(q_i)$ for the invariant mass of the $c\bar{c}$ pair for the nonfragmentation diagram, the authors of Ref. [23] used the physical mass $m_{J/\psi}$ to normalize the heavy-quarkonium state. Another source of the difference is that we use $\alpha = 1/132.6$ to determine $g_{J/\psi}$, whose scale is taken to be $m_{J/\psi}$, but in Ref. [23], $\alpha = 1/137$ was used.

We notice that the LO cross section $\sigma_0^{\rm fr}$ in Table III is significantly smaller than σ_0 shown in Table II. This is because the relativistic corrections to all orders in v are already included in the fragmentation contribution to $\sigma_0^{\rm fr}$ that was computed with the VMD approach. In addition, $\sigma_{v^\infty}^{\rm fr}$ and $\sigma_{v^2}^{\rm fr}$ are essentially the same as $\sigma_0^{\rm fr}$. As a result, $K_{v^\infty}^{\rm fr} \approx K_{v^2}^{\rm fr} \approx 1$. This indicates that the relativistic correction to the contribution not coming from photon fragmentation is negligible.

It is important to notice that, in the VMD approach, the QCD and relativistic corrections to the photon-J/ψ vertex have been effectively resummed to all orders. Therefore, one must be careful to avoid double counting of the QCD NLO corrections when one combines the NRQCD one-loop corrections and the relativistic corrections. In each photon-J/ψ vertex of the photon-fragmentation diagrams, there is a QCD NLO correction factor $[1 - 16\alpha_s/(3\pi)]$ at the cross-section level. Therefore, in order to subtract the amount that is contained in the NRQCD one-loop corrections in Ref. [22], we add $32\alpha_s/(3\pi)$ to the factor K_{α_s} extracted from the result in Ref. [22]. The resultant factor is very close to 1: $K^{\rm fr}_{\alpha_s} = 0.944$ (0.939), 0.964 (0.956), and 0.969 (0.964) for $\mu = m_c$, $2m_c$, and $\sqrt{s}/2$, respectively, at $m_c = 1.4$ (1.5) GeV.

Because most of the QCD and relativistic corrections are already contained in $\sigma^{\rm fr}_0$, we have found that $K^{\rm fr}_{\alpha_s} \approx 1$ and $K^{\rm fr}_{v\infty} \approx 1$. In this limit, the interference between the QCD and relativistic corrections is negligible. Therefore, we take $\sigma^{\rm fr}_{\rm tot} \approx K^{\rm fr}_{v\infty}\sigma^{\rm fr}_0 + (K^{\rm fr}_{\alpha_s} - 1)\sigma_0$. The results for $\sigma^{\rm fr}_{\rm tot}$ are listed on the last three columns of Table III. It is remarkable that every entry for $\sigma^{\rm fr}_{\rm tot}$ listed in Table III is positive in contrast to the corresponding values in Table II. This is a strong indication that the corrections of order higher than $\alpha_s v^0$ may resolve the problem that the NRQCD prediction gives negative cross section. In addition, $\sigma^{\rm fr}_{\rm tot}$ is insensitive to the variation of the scale μ from m_c to $\sqrt{s}/2$. Our prediction for $\sigma^{\rm fr}_{\rm tot}$ is consistent with the nonobservation of the process at Belle with an upper bound $\sigma[e^+e^- \to J/\psi + J/\psi] \times \mathcal{B}_{>2}[J/\psi] < 9.1\,{\rm fb}$ [6].

V. CONCLUSION

We have computed the cross sections for the two exclusive production processes, $e^+e^- \to \eta_c + \gamma$ and $e^+e^- \to J/\psi + J/\psi$ at $\sqrt{s} = 10.58$ GeV, in which a class of relativistic corrections are resummed to all orders in v. By including the available QCD corrections of order α_s and the interference between the QCD and resummed relativistic corrections, we further improved the corresponding theoretical predictions.

The NRQCD prediction for the cross section of $e^+e^- \to \eta_c + \gamma$ is listed in Table I. The value $\sigma_{\rm tot} \approx 50\,{\rm fb}$, that is about 60–70 % of the LO cross section σ_0, contains the QCD NLO and resummed relativistic corrections, and their interference. In this process, both the QCD NLO and order-v^2 relativistic corrections are negative. The relativistic corrections of order-v^4 or higher are negligible. The value for $\sigma_{\rm tot}$ is still large enough to be measured at B factories or super B factories, for example, through the $\eta_c \to K\bar{K}\pi$ decay mode.

In the case of $e^+e^- \to J/\psi + J/\psi$, which is dominated by the photon fragmentation, we have found that the standard NRQCD prediction for $\sigma_{\rm tot}$, shown in Table II, is negative for every choice of input parameters. As an alternative, we have employed the VMD approach to include the QCD and relativistic corrections to the photon-J/ψ vertex in the photon-fragmentation diagrams. The VMD result $\sigma_{\rm tot}^{\rm fr} \approx 1\,{\rm fb}$, given in Table III, indeed resolves the problem of negative cross section and the prediction is insensitive to the scale μ. This is a strong indication that corrections of order higher than $\alpha_s v^0$ may have significant contributions. The predicted cross section for $e^+e^- \to J/\psi + J/\psi$ is consistent with the nonobservation of the events at Belle.

Acknowledgments

Y.F. would like to express appreciation to Korea Institute for Advanced Study (KIAS) for its hospitality while a part of this work was carried out. We thank KIAS Center for Advanced Computation for providing us with the Abacus2 System. The work of C.Y. was supported in part by Basic Science Research Program through the National Research Foundation of Korea (NRF) funded by the Ministry of Education Science and Technology (2011-0022996) and by NRF Research Grant No. 2012R1A2A1A01006053. The work of J.L. was supported by the NRF under the Grant No. 2009-0070667.

[1] G. T. Bodwin, E. Braaten, and G. P. Lepage, Phys. Rev. D **51**, 1125 (1995) [Erratum-ibid. D **55**, 5853 (1997)] [hep-ph/9407339].

[2] G. T. Bodwin, X. Garcia i Tormo, and J. Lee, Phys. Rev. Lett. **101**, 102002 (2008) [arXiv:0805.3876 [hep-ph]]; Phys. Rev. D **81**, 114005 (2010) [arXiv:0903.0569 [hep-ph]]; Phys. Rev. D **81**, 114014 (2010) [arXiv:1003.0061 [hep-ph]].

[3] K. Abe *et al.* [Belle Collaboration], Phys. Rev. Lett. **89**, 142001 (2002) [hep-ex/0205104].

[4] E. Braaten and J. Lee, Phys. Rev. D **67**, 054007 (2003) [Erratum-ibid. D **72**, 099901 (2005)] [hep-ph/0211085].

[5] K.-Y. Liu, Z.-G. He, and K.-T. Chao, Phys. Lett. B **557**, 45 (2003) [hep-ph/0211181].

[6] K. Abe *et al.* [Belle Collaboration], Phys. Rev. D **70**, 071102 (2004) [hep-ex/0407009].

[7] B. Aubert *et al.* [BABAR Collaboration], Phys. Rev. D **72**, 031101 (2005) [hep-ex/0506062].

[8] Y.-J. Zhang, Y.-j. Gao, and K.-T. Chao, Phys. Rev. Lett. **96**, 092001 (2006) [hep-ph/0506076];

B. Gong and J.-X. Wang, Phys. Rev. D **77**, 054028 (2008) [arXiv:0712.4220 [hep-ph]].

[9] G. T. Bodwin, D. Kang, and J. Lee, Phys. Rev. D **74**, 114028 (2006) [hep-ph/0603185].

[10] G. T. Bodwin, D. Kang, and J. Lee, Phys. Rev. D **74**, 014014 (2006) [hep-ph/0603186].

[11] G. T. Bodwin, J. Lee, and C. Yu, Phys. Rev. D **77**, 094018 (2008) [arXiv:0710.0995 [hep-ph]].

[12] G. T. Bodwin, D. Kang, T. Kim, J. Lee, and C. Yu, AIP Conf. Proc. **892**, 315 (2007) [hep-ph/0611002].

[13] Z.-G. He, Y. Fan, and K.-T. Chao, Phys. Rev. D **75**, 074011 (2007) [hep-ph/0702239 [HEP-PH]].

[14] H.-R. Dong, F. Feng, and Y. Jia, Phys. Rev. D **85**, 114018 (2012) [arXiv:1204.4128 [hep-ph]].

[15] G. T. Bodwin, H. S. Chung, D. Kang, J. Lee, and C. Yu, Phys. Rev. D **77**, 094017 (2008) [arXiv:0710.0994 [hep-ph]].

[16] G. T. Bodwin, H. S. Chung, J. Lee, and C. Yu, Phys. Rev. D **79**, 014007 (2009) [arXiv:0807.2634 [hep-ph]].

[17] H. S. Chung, J. Lee, and C. Yu, Phys. Lett. B **697**, 48 (2011) [arXiv:1011.1554 [hep-ph]].

[18] H.-K. Guo, Y.-Q. Ma, and K.-T. Chao, Phys. Rev. D **83**, 114038 (2011) [arXiv:1104.3138 [hep-ph]].

[19] E. Braaten, B. A. Kniehl, and J. Lee, Phys. Rev. D **62**, 094005 (2000) [arXiv:hep-ph/9911436]; M. Butenschoen and B. A. Kniehl, Phys. Rev. D **84**, 051501 (2011) [arXiv:1105.0820 [hep-ph]]; Y.-Q. Ma, K. Wang, and K.-T. Chao, Phys. Rev. D **84**, 114001 (2011) [arXiv:1012.1030 [hep-ph]].

[20] G. T. Bodwin, J. Lee, and E. Braaten, Phys. Rev. Lett. **90**, 162001 (2003) [Erratum-ibid. **95**, 239901 (2005)] [hep-ph/0212181].

[21] G. T. Bodwin, J. Lee, and E. Braaten, Phys. Rev. D **67**, 054023 (2003) [Erratum-ibid. D **72**, 099904 (2005)] [hep-ph/0212352].

[22] B. Gong and J.-X. Wang, Phys. Rev. Lett. **100**, 181803 (2008) [arXiv:0801.0648 [hep-ph]].

[23] G. T. Bodwin, E. Braaten, J. Lee, and C. Yu, Phys. Rev. D **74**, 074014 (2006) [hep-ph/0608200].

[24] H. S. Chung, J. Lee, and C. Yu, Phys. Rev. D **78**, 074022 (2008) [arXiv:0808.1625 [hep-ph]].

[25] W.-L. Sang and Y.-Q. Chen, Phys. Rev. D **81**, 034028 (2010) [arXiv:0910.4071 [hep-ph]].

[26] D. Li, Z.-G. He, and K.-T. Chao, Phys. Rev. D **80**, 114014 (2009) [arXiv:0910.4155 [hep-ph]].

[27] G. T. Bodwin, U-R. Kim, and J. Lee, JHEP **11**, 020 (2012) [arXiv:1208.5301 [hep-ph]].

[28] G. T. Bodwin and A. Petrelli, Phys. Rev. D **66**, 094011 (2002) [hep-ph/0205210].

[29] M. Gremm and A. Kapustin, Phys. Lett. B **407**, 323 (1997) [hep-ph/9701353].

[30] Y. Fan, J. Lee, and C. Yu, arXiv:1209.1875 [hep-ph].

[31] Z.-G. He, R. Li, and J.-X. Wang, Phys. Lett. B **711**, 371 (2012) [arXiv:0904.1477 [hep-ph]].

[32] J. Lee, W. Sang, and S. Kim, JHEP **1101**, 113 (2011) [arXiv:1011.2274 [hep-ph]].

[33] Y. Jia, X.-T. Yang, W.-L. Sang, and J. Xu, JHEP **1106**, 097 (2011) [arXiv:1104.1418 [hep-ph]];

[34] J.-Z. Li, Y.-Q. Ma, and K.-T. Chao, arXiv:1209.4011 [hep-ph].

[35] F. Feng, Y. Jia, and W.-L. Sang, arXiv:1210.6337 [hep-ph].

[36] J. Beringer *et al.* [Particle Data Group Collaboration], Phys. Rev. D **86**, 010001 (2012).